Modular approach to fabrication of three-dimensional microchannel systems in PDMS - Application to sheath flow microchips

ARTICLE *in* LAB ON A CHIP · JANUARY 2002

Impact Factor: 6.12 · DOI: 10.1039/b105110p · Source: PubMed

3 AUTHORS, INCLUDING:

Philippe Niedermann
Centre Suisse d'Electronique et de Microtec…
127 PUBLICATIONS **1,631** CITATIONS
SEE PROFILE

Andreas Manz
Korea Institute of Science and Technology …
305 PUBLICATIONS **19,502** CITATIONS
SEE PROFILE

LAB ON A CHIP

Modular approach to fabrication of three-dimensional microchannel systems in PDMS—application to sheath flow microchips

Oliver Hofmann,[a] Philippe Niedermann[b] and Andreas Manz*[a]

[a] *AstraZeneca/SmithKline Beecham Centre for Analytical Science, Imperial College of Science, Technology & Medicine, Exhibition Road, London, UK SW7 2AY*
[b] *CSEM Centre Suisse d'Electronique et de Microtechnique SA, Rue Jaquet-Droz 1 CH-2007. Neuchatel, Switzerland*

Received 11th June 2001, Accepted 2nd October 2001
First published as an Advance Article on the web 15th November 2001

A modular approach to fabrication of three-dimensional microchannel systems in polydimethylsiloxane (PDMS) is presented. It is based on building blocks with microstructuring on up to three faces. The assembled 3D-microchip consists of three building blocks in two layers. For assembly of the bottom layer two building blocks are joined horizontally, whereby the side structuring of the first is sealed against the flat side surface of the other. This results in the formation of a vertical interconnection opening between the building blocks to supplement the microstructuring on the lower faces. The 3D microchannel system is completed by placing a third building block, with microstructuring only on its lower face, on top of the assembled layer. While plasma assisted bonding is used between the two building blocks of the bottom layer, inherent adhesion is sufficient between the layers and for attaching the assembled 3D-microchip to a substrate. This modular approach was applied to the fabrication of a 3D-sheath flow microchip. It comprises a 20 μm deep microchannel system with sample inlet, open sensing area and outlet in the bottom layer and sheath flow inlet in the top layer. 100 μM fluorescein at 6 μL min^{-1} was used as sample flow and water at increasing flow rates as sheath flow. With ratios of sheath to sample flow up to 20 : 1 sample layers down to 1 μm thickness could be generated. Sample layer thickness was determined *via* volume detection on an epi-fluorescence microscope followed by image analysis.

Introduction

Over the last two decades, intensive work has been directed towards miniaturisation of analytical methods.[1–5] Technologies previously used in the fabrication of integrated circuits have successfully been transferred to this domain.[6] This has enabled fabrication of integrated analytical devices and micro total analysis systems (μTAS).[7,8] Until recently, most devices have been fabricated in silicon or glass comprising two-dimensional channel systems. Only a few three-dimensional microfluidic devices have been reported such as a stacked multilayer silicon structure,[9] or an interconnecting structure fabricated by joining of two silicon substrates with anisotropically etched cavities.[10] Typically these silicon or glass based approaches require complex micromachining, have constraints in structuring in the third dimension, and require O-rings and clamping force for sealing. A fundamentally different approach is microstereolithography with which three-dimensional structures can be fabricated directly. Micro-mechanical components consisting of up to 1000 layers of 5 μm thickness were fabricated by Bertsch *et al.*[11] However, application of this technique to fabrication of 3D-microfluidic structures is currently hampered by the lack of suitable starting materials with photon polymerisation initiators.[12]

Over the last five years a new trend towards elastomeric materials and molding techniques has developed. The elastomer most commonly used is polydimethylsiloxane (PDMS). This has favourable optical properties and exhibits interfacial adhesion that benefits bonding.[13] Molding requires casting from a master with a corresponding surface relief. For PDMS molding a variety of masters have been employed including structured glass, structured silicon,[14–16] and structured photoresist on a silicon support.[17–20] PDMS microchips seal reversibly when brought into conformal contact with a variety of flat substrates,[21] including glass,[15,18,20,22] silicon,[18] waveguiding layers,[23] and PDMS itself.[14,16,19,20] To obtain a permanent bond the surfaces to be joined can be treated with an oxygen plasma.[19] This has the additional benefit of temporarily increased hydrophilicity of the channels, facilitating their filling with aqueous liquids.[18,19,22,24]

PDMS molding requires the fabricated piece to be peeled off the master after curing. Therefore, complex 3D-devices with multiple level microchannel structuring cannot directly be realised with this method. However, this limitation can be overcome by assembly approaches. One approach is to stack several thin layers of PDMS containing two-dimensional channel structures and through-holes, as has been described by Beebe *et al.*[25,26] To fabricate the layers, a sandwich molding process is used in which PDMS is cured between a two-level SU-8 master and a transparency film clamped against it, with the layer thickness defined by the surface structure on the master. Since SU-8 masters are fabricated photolithographically the structuring in the third dimension can only consist of through-holes without sub-structure. The resulting thin layers of PDMS are difficult to peel off and handling in the stacking step is delicate. A more sophisticated approach to fabricate topologically complex three-dimensional microstructures in PDMS has been pioneered by Whitesides *et al.*[27,28] PDMS layers with already three-dimensional structuring are used for stacking. The structuring consists of channels on each face of the layer and interconnections between them. To fabricate the 3D-layers a sandwich molding process is used in which PDMS is cured between a two-level SU-8 master and a PDMS master, also with two-level structuring, is clamped against it. This approach

 DOI: 10.1039/b105110p

suffers from the same constraints on structuring in the third dimension as the approach of Beebe *et al.*[25,26] Sub-structuring of the through-holes is not feasible within one layer.

Here we present a modular PDMS-molding approach with virtually no constraints on structuring in the third dimension. Individual building blocks are fabricated by PDMS molding from up to three silicon masters arranged in a special molding dish. This enables alignment of microstructures across several faces of the building block with micrometer precision. A three dimensional microchannel system is realised through the assembly of three building blocks forming two layers. The thickness of the bottom layer building blocks is determined by the size of the master chips used for side structuring. Typically, the building blocks are several millimetres thick. This facilitates their handling and benefits durability. The aspect ratio that can be obtained for the side structuring, which translates to the third dimension after microchip assembly, is defined by the surface structure on the master chip.

This modular approach was applied to the fabrication of 3D-microchips for sheath flow applications. Sheath flows are commonly used in flow cytometry. In the standard configuration, sample flow is introduced into the centre of a flowing sheath stream and guided past a detector.[29,30] Biological samples can be manipulated such that a thin stream of individual particles is generated, *e.g.* for cell counting *via* light scattering detection. Recently, Shoji *et al.* have developed a chip based flow cell for biomolecule and particle handling incorporating 3D-sheath flow.[31] In this configuration the sample flow is introduced through a small inlet located between two larger sheath flow inlets. The resulting envelope of sheath flow minimizes exposure of the sample flow to the channel walls to avoid adsorption effects.

Here we report on a sheath flow configuration aimed at confining sample flow to the vicinity of a substrate surface. This can be used to enhance mass transport to sensor surfaces as described elsewhere.[32,33] While this configuration has been proposed before by Duveneck *et al.* their paper does not provide experimental validation.[34] In our arrangement a sample flow is joined with a perpendicular sheath flow introduced through a microstructured slit in the upper wall of the sample inlet channel. By using a slit rather than through holes a larger area can be supplied with the double flux of sample and sheath flow. A further advantage of the slit configuration is the resulting uniform flow resistance throughout the flow cell.

Other applications for the modular 3D fabrication approach could include laminar micromixers, microchannel separation systems with high sensitivity absorbance detection (with vertical extension to increase the optical path length), or μTAS devices.

Experimental

A new building block approach is presented in which three-dimensional microstructures can be obtained within one microchip layer. By joining two PDMS pieces horizontally with one of them microstructured not only on its lower face but also on one side surface, an interconnection cavity can be formed between them. Placing a third PDMS piece, microstructured only on its lower face, on top of the joined layer results in an interconnected two-layer system (Fig. 1).

Channel layout

Following this modular approach a 3D-microchip for sheath flow applications was fabricated. It comprised a 20 μm deep microchannel system with sample inlet, open sensing area and outlet in the bottom layer and sheath flow inlet in the top layer. It was designed for application to evanescent wave bio-sensors.[32] A branching channel structure[35] was used to distribute flow uniformly over the 10 × 6 mm sensing area. 100 μm wide spacers in the interconnection opening and 20 μm diameter posts in the sensing area, spaced evenly at 200 μm, were integrated into the layout for structural support.

Silicon master

A silicon master was diced into master chips comprising segments of the channel layout. A positive surface relief was obtained *via* reactive ion etch in an inductively coupled plasma (ICP-RIE).

Molding of building blocks from multiple silicon masters

To facilitate PDMS peeling-off after curing, all master chips were silanised with dimethyloctylchlorosilane for two hours, followed by rinses with toluene and water.[14]

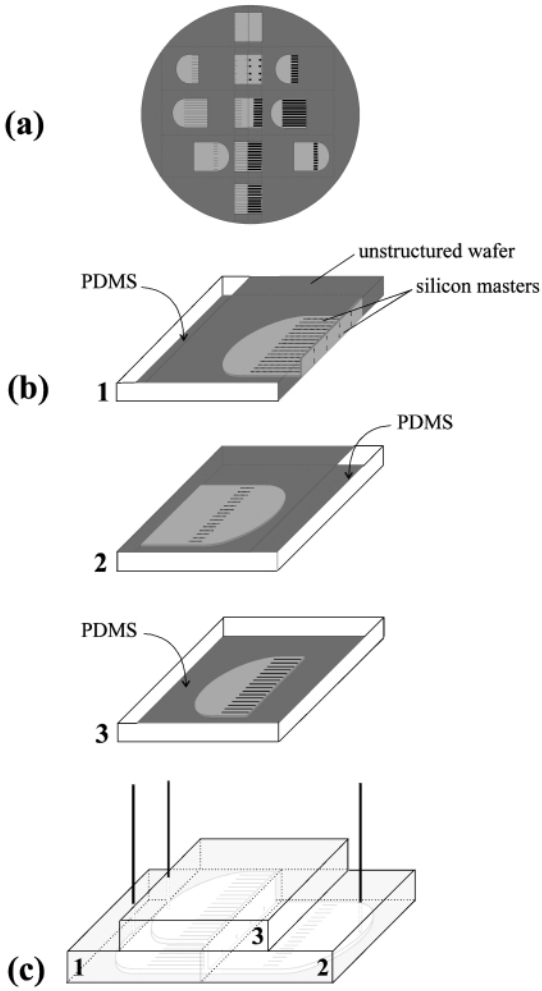

Fig. 1 Modular approach to fabrication of 3D-microchips based on horizontal and vertical assembly of molded PDMS building blocks. (a) Silicon master comprising segments of the 3D-microchip layout is cut into individual master chips. (b) PDMS-molding of building blocks. For building block 1, master chips comprising sample flow inlet and interconnection are joined in a perpendicular orientation and an un-structured silicon wafer is placed on top (1). For building block 2, a master chip comprising the sensor cell outlet is joined with un unstructured silicon chip in perpendicular orientation, again with an unstructured silicon wafer placed on top (2). The third building block is molded from just one master chip with sheath flow inlet (3). After pouring and curing of the PDMS, the building blocks are pealed off and the edges are trimmed. (c) Assembly of a two-layer, three-piece 3D-microchip with punched inlet and outlet holes and inserted capillaries serving as fluidic connectors.

For molding, a special dish for alignment and joining of up to three master chips was designed and made from aluminium (Fig. 2). Essential components are a molding dish base, a slider, and two positioning screws. For molding of building block 1 of the 3D-microchip the first master was fixed horizontally in the base with double-sided sticky tape (Scotch #11278, 3M). The second master was prefixed to the vertical surface of the slider with sticky tape, positioned, and then permanently fixed with epoxy adhesive (AY105 and HY 991, Araldit). The fixation typically lasted for several molding runs. For joining master 2 with the surface structure of master 1 the slider was moved along one sidewall of the molding dish base with a Teflon inlet on the other side providing additional support. While the *x*-positioning screw was used to move the slider the *y*-positioning screw was tightened to keep the slider pressed against the sidewall of the molding dish base. This ensured a parallel orientation of the edges of masters 1 and 2, as required for proper joining. After joining an unstructured silicon wafer was placed on top of the vertical master 2. To ensure conformal contact between the two masters the *z*-fixation screw was tightened, pressing the unstructured wafer from top against master 2 and the parallel master 1. Finally, PDMS elastomer and curing agent were mixed at a ratio of 10 : 1 w/w, degassed for 30 min, poured into the molding dish base and cured at 95 °C for 1 h. After curing, the unstructured silicon wafer was removed and the PDMS piece peeled off. The non-microstructured sides were then trimmed with a scalpel to ensure flat surfaces for assembly.

For molding of building block 2 an unstructured silicon wafer could be used instead of master 2. To obtain an interconnection opening in the assembled bottom layer of the 3D-microchip, a microstructured side surface is required on only one building block.

Fabrication of building block 3 required only one master, which was mounted horizontally in the molding dish base.

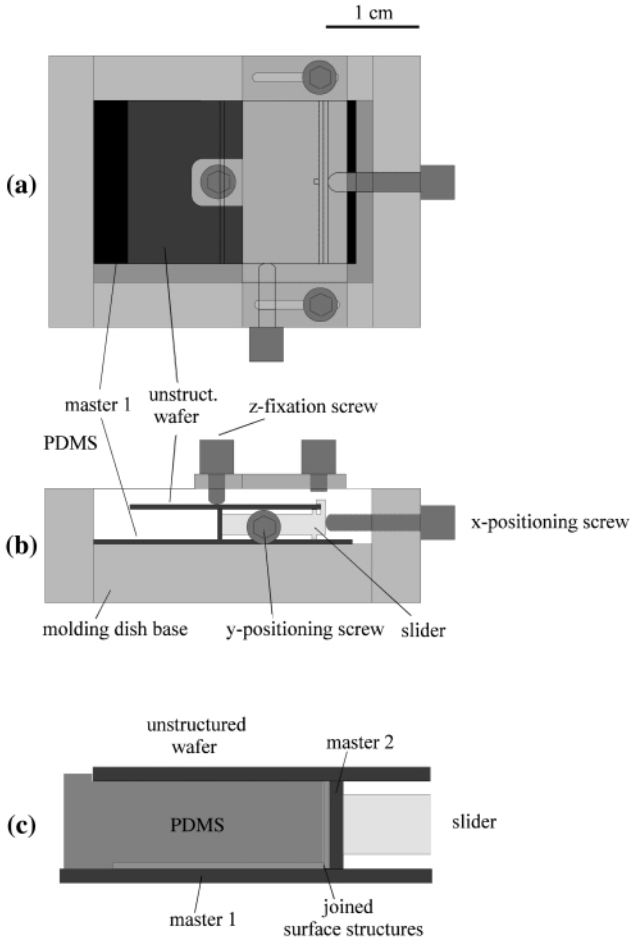

Fig. 2 Dish for molding from multiple joined master chips. Arrangement as for fabrication of building blocks 1 or 2. Joining operation is described in the text. (a) Top view of the molding dish base. (b) Side view of the molding dish base. (c) Enlargement of the master arrangement after joining of the surface structures.

Assembly of 3D-microchip

The PDMS building blocks comprising sample flow inlet and interconnection (1 in Fig. 3), and sensor cell and outlet (2 in Fig. 3) were joined first to form the bottom layer of the 3D-microchip. This was performed on a polished ceramic plate with an alignment precision of ±20 μm. The PDMS building block comprising the sheath flow inlet (3 in Fig. 3) was then placed on top of the joined bottom layer. With a simple customized micromanipulator an alignment precision similar to the one for joining of the bottom layer could be obtained. Between the two pieces of the bottom layer only a small surface area is available for bonding (approximately 10 mm^2 on each side, depending on trimming). To get a strong, permanent bond, plasma treatment was applied.[19] The assembly procedure was typically completed within 5 min, with yields of around 90%.

The main advantage of using inherent adhesion between the bottom and top layer and for substrate attachment is that cleaning and reuse of the 3D-PDMS microchip is greatly facilitated. At the same time the permanent bond around the critical interconnection in the bottom layer ensures sufficient mechanical stability and durability of the assembled microchip.

For channel access holes were punched with a syringe needle (394 μm id, 711 μm od). Capillaries (150 μm id, 375 μm od) were then inserted from the structured side of the PDMS to serve as fluidic connectors. The adhesive-free fixation of the connectors again benefits cleaning of the microchip. A schematic of the assembled 3D-microchip is given in Fig. 3.

It should be stressed that the described molding and assembly procedures were only aimed at fabricating 3D-microchip prototypes for research. For fabricating larger numbers the individual building blocks could be injection molded. Layout integrated alignment tracks could be employed to further facilitate chip assembly.

Filling procedure

Untreated PDMS is highly hydrophobic resulting in poor wetting with high surface tension liquids such as water. Filling of channel systems in PDMS is therefore difficult and bubble formation is common.[19] For three-dimensional channel sys-

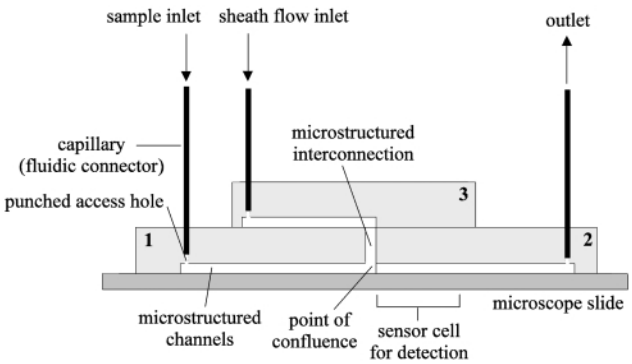

Fig. 3 Schematic of the assembled sheath flow 3D-microchip. The interconnection between the microchannels in the top and bottom layer of the microchip corresponds to the side structuring of building block 1 sealed against the flat side surface of building block 2. Bonding between the building blocks and sealing around the capillary connectors is non-adhesive based.

tems, filling can be even more problematic. Typically accessibility is limited and there are higher dead volumes. One approach to facilitate filling is to decrease the surface tension of the filling liquid. This approach was taken and optimised for Tween 20, with best results obtained for 0.1% v/v. Complete filling could be achieved within less than 1 min. All solutions were degassed for 10 min in an ultrasonication bath and filtered with 0.45 μm pore size syringe filters prior to use.

Set-up for flow visualisation

An inverted fluorescence microscope (DMIL, Leica) with incident light illumination was used for all flow visualisation experiments. A CCD camera mounted to a phototube (FSA/20, Leica) was employed for recording sequences on video tape. CCD detection with subsequent image capture and analysis was preferred over detection with a photo-multiplier tube because local fluorescence intensities can be derived. For all flow visualization experiments the 3D-microchip was assembled on a glass microscope slide. Flexible PTFE tubing with 350 μm id was used to connect the sample and sheath flow inlets to Kloehn syringe pumps (syringe drive modules 50300, Kloehn). The pumps were computer controlled *via* a multifunction data acquisition card (PCI-MIO-16E-4, National Instruments) and Labview software.

Layer thickness determination with Scion imaging analysis

Individual frames of the video sequences were captured and analysed with Scion imaging software. A calibration with fluorescein solutions was performed to validate a correlation between the Scion imaging reading and fluorescence intensity, and to determine the linear range. The Scion imaging reading for 100 μM fluorescein filling the whole channel was used as a reference for full fluorescence or a layer thickness of 20 μm (internal standard 0) while the reading for water served as a reference for no fluorescence or a layer thickness of 0 μm (internal standard 1). For sheath flow experiments with a double layer of 100 μM fluorescein and water the thickness of the fluorescein layer was calculated by linear regression between the two references.

Results and discussion

Quality assessment of the 3D-microchip

PDMS building blocks with a proper imprint of the silicon master structures and planar surfaces on three sides have successfully been fabricated and assembled to construct a 3D-microchip. Building block 1 with sample flow inlet and interconnection microstructuring is depicted in Fig. 4. The top half of the image shows 200 × 20 μm sample inlet channels separated by 100 μm wide supporting walls. In the bottom half a 20 μm deep interconnection cavity and a 100 μm wide spacer can be seen. Upon assembly of the 3D-sheath flow microchip, this cavity interconnects the sample inlet channels on the lower face of building block 1 with the sheath flow inlet channels in the top layer. Spacers are required to prevent closing of the interconnection through deformation of the PDMS. The fabrication of such a substructure in the vertical plane nicely demonstrates the 3D-capabilities of our molding based assembly approach.

Fig. 5 depicts plasma-bonded building blocks 1 and 2 forming the bottom layer of the 3D-microchip. In (a) the sample inlet channels can be seen in the top half of the images and the sensor cell with the array of 20 μm diameter posts in the bottom half. The imperfection towards the right end of the sensor cell is due to a chipped-off surface structure on the master used for molding. A slight misalignment of approximately 20 μm can be observed at the side ends of the interconnection. The plasma-enhanced bonding proved to be very robust. A 3D-microchip with plasma-bonded bottom layer was used for approximately fifty experiments over the course of one year without any observable weakening of the bond.

Sheath flow testing

In our sheath flow configuration a sample flow is confined to the vicinity of a substrate surface through the introduction of a

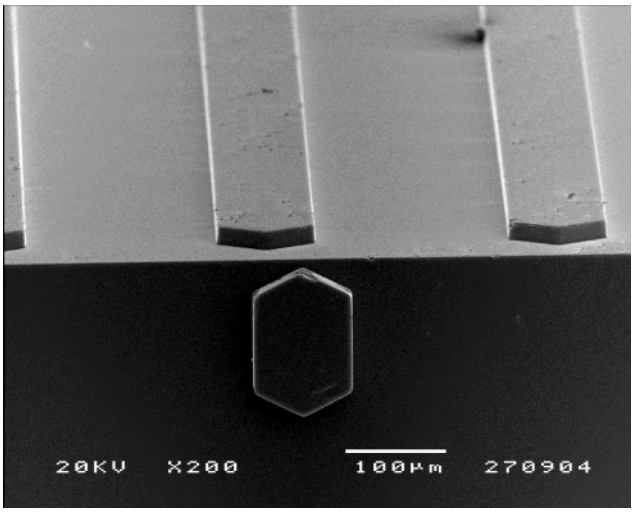

Fig. 4 Scanning electron micrograph of PDMS building block 1. At the top, 200 × 20 μm sample inlet channels separated by 100 μm wide supporting walls are shown. The examined section corresponds to the end of the branching channel structure aimed at distributing sample flow uniformly over the sensing area. The bottom half shows a 20 μm deep cavity with an integrated 100 μm wide spacer. Upon assembly of all three building blocks this opening interconnects the two layers of the 3D-microchip.

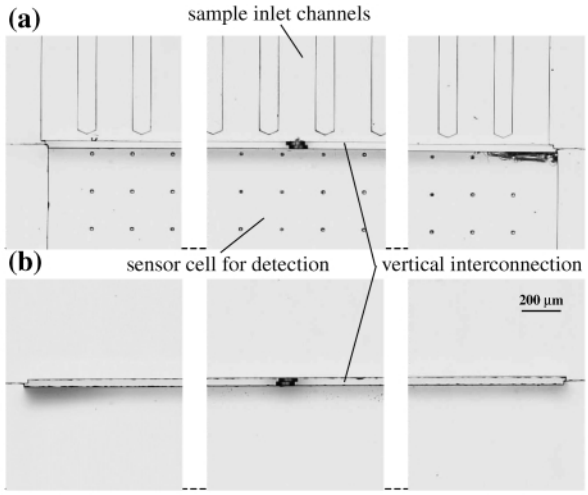

Fig. 5 Optical micrographs of the bottom layer of the 3D-microchip, assembled from building blocks comprising sample inlet and interconnection (building block 1), and sensor cell outlet (building block 2). The surfaces around the interconnection were plasma-treated prior to joining resulting in permanent bond formation. (a) and (b) show the views from the bottom and the top, respectively. The interconnection can be seen as a slit.

perpendicular sheath flow, as illustrated in Fig. 6. To determine the thickness of the generated sample layer, a simple procedure was developed. Since a confocal microscope with sufficiently high resolution (low micrometer range) was not available, volume detection with a conventional epi-fluorescence microscope was tested. For this to yield quantitative results two criteria have to be met. (i) Excitation and detection of emitted light has to be uniform across the whole channel. (ii) The concentration of the fluorescing sample solution has to be sufficiently low to avoid reabsorption of fluorescence light (inner filter effect).[36] For (i) the depth of field has to be greater than the channel depth. While in light microscopy the depth of field determines the thickness of a layer that yields a reasonably sharp image, in sheath flow experiments with epi-illumination it determines the thickness of a layer in which excitation light is well focused and collection of the emitted fluorescence light

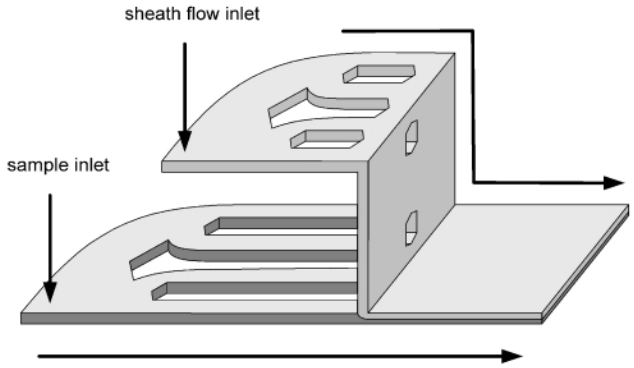

Fig. 6 Schematic of sheath flow operation with the 3D-microchip. Sample and sheath flows are introduced through a branching channel system for uniform distribution of the flows over a wide area. The sample flow is joined with the sheath flow from the top layer of the 3D-microchip through an interconnection. After confluence a double flux of sample and sheath flow in a planar sheet geometry is obtained. This double flux can be detected in the sensor cell.

efficient. For the 2.5× objective used a depth of field of approximately 52 μm can be calculated (using the formula given in ref. 37) This is well above the channel depth of 20 μm. For (ii) the concentration range in which fluorescence is directly proportional to absorption was determined by flushing a series of fluorescein solutions with concentrations between 100 nM and 2.5 mM through the 3D-microchip. The linear range (Lambert–Beer region) was found to be between 5 and 250 μM with a linear correlation coefficient, R^2, of 0.998. For sheath flow experiments with increasingly thin layers of fluorescein being detected this corresponds to a detection limit of 100 μM fluorescein filling one twentieth of the channel depth or a layer of 1 μm. However, it has to be stressed that this volume detection method cannot distinguish between a fluorescein–water double layer and a solution mixed accordingly. Even under laminar conditions, as used in these experiments, diffusional mixing occurs at the flow interface. For 10 : 1 sheath flow and the 2 mm section of the sensing area analysed an average diffusion path length of 19 μm can be calculated (based on transit time 0.4 s, diffusion coefficient 5×10^{-10} m^2 s^{-1}). Considering the channel depth of 20 μm and an expected sample layer thickness of approximately 4 μm this is significant. The determined values for sample layer thickness are therefore only valid for the area immediately downstream of the point of confluence between sample and sheath flow. This method measures an effective thickness, with the precision given by the fluorescence quantification. Because of the good linearity of the latter, the precision is deemed sufficient for the present application.

The experimental series was started with 100 μM fluorescein solution at the sample inlet at 6 μL min^{-1} (internal standard 0), with the objective focused between channel top and bottom of the sensor cell. The second sequence was deionised water at the sheath flow inlet at 6 μL min^{-1} (internal standard 1). For sheath flow experiments the fluorescein flow rate was kept constant at 6 μL min^{-1} and the sheath flow rate was increased in multiples of the sample flow rate. This was continued until leakage occurred yielding additional valuable information about max-

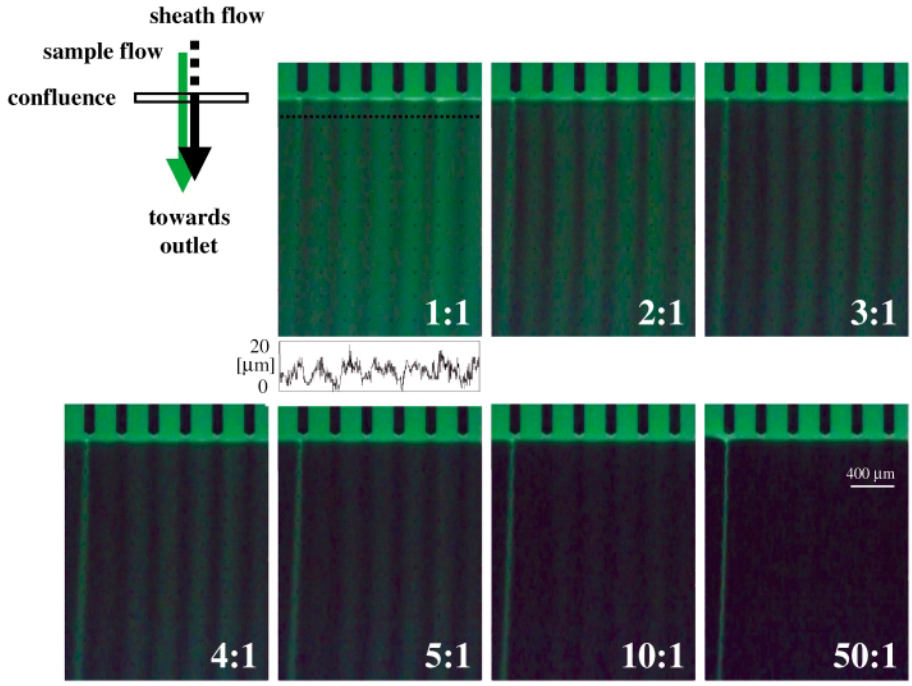

Fig. 7 Flow patterns under sheath flow conditions. Sample flow (100 μM fluorescein): 6 μL min^{-1}. Sheath flow (water): 6–300 μL min^{-1}. Numbers correspond to ratio of sheath to sample flow. Images were acquired at 2.5× magnification. Brightness and contrast were adjusted for better viewing. For 1 : 1 flow confinement a fluorescence intensity profile is also displayed. It was taken approximately 100 μm downstream of the point of confluence between sheath and sample flow, as indicated in the image. Noise reduction was *via* rank filtering (each centre pixel of a 3 × 3 neighbourhood is replaced by the median value). For sample layer thickness calibration, internal standards 0 and 1 were used, as described in the text.

imum flows that can be applied to the 3D-microchip. Flow rates of 120 μL min^{-1} were routinely applied without sealing problems. This corresponds to a linear velocity of 1 cm s^{-1} over the sensor surface or a transit time of 0.6 s. Leakage typically occurred for flows in excess of 300 μL min^{-1} (2.5 cm s^{-1}).

Typical flow patterns for a series of different sheath flow rates are depicted in Fig. 7. The images represent a view from underneath through the microscope slide onto the channel structure of the 3D-microchip sealed against it. The sample inlet channels can be seen at the top separated by supporting walls (dark areas). Perpendicular to the ends of the sample inlet channels is a 40 μm wide interconnection opening through which the sheath flow enters from the top layer of the 3D-microchip. Below the interconnection is the open sensor cell supported by 20 μm diameter posts, spaced at 200 μm. Flow direction is from top to bottom towards the common outlet of sample and sheath flow (not shown).

The channel walls of the sample inlet are close enough to the junction with the sheath flow to influence the flow pattern after confluence, leading to the observed lowered fluorescence downstream of the walls. This renders the flow pattern visible, and the flow lines are confirmed to be straight and thus the flow velocities uniform across all of the sensor cell, which is a consequence of the symmetrical branching channel layout. An isolated sharp flow line of higher fluorescence intensity can be observed towards the left side of the sensor cell. We attribute this to an imperfection or a dust particle in the corresponding section of the interconnection resulting in locally suppressed sheath flow.

With increasing sheath flow rate there is a clear decrease of fluorescence intensity in the sensor cell, as is expected for the two layer flow. From profiles of the fluorescence intensity across the sensor cell it can be seen that for 1 : 1 flow confinement sample layer thickness varies between approximately 15 and 5 μm, with lower thickness obtained downstream of the walls separating the sample inlet channels. For 2 : 1 flow confinement the sample layer thickness is reduced to between approximately 10 and 5 μm. With flow confinement increased to 5 : 1 and 10 : 1, sample layers are confined to thicknesses below 5 and 4 μm, respectively, with areas downstream of the walls confined to layer thicknesses below the detection limit (not shown). When the whole sensor cell area is analysed this results in an average sample layer thickness that decreases continuously as a function of the sheath flow rate (Fig. 8). The values represent the average of three runs performed on different days with the same 3D-microchip. For 1 : 1 and 10 : 1 flow confinement average sample layers of 11.4 ± 1.1 μm and 1.8 ± 0.4 μm are obtained, respectively. For all flow confinements higher than 1 : 1 standard deviations are below ±1 μm. This shows that the sheath flow experiments and the approach of sample layer thickness determination are reproducible.

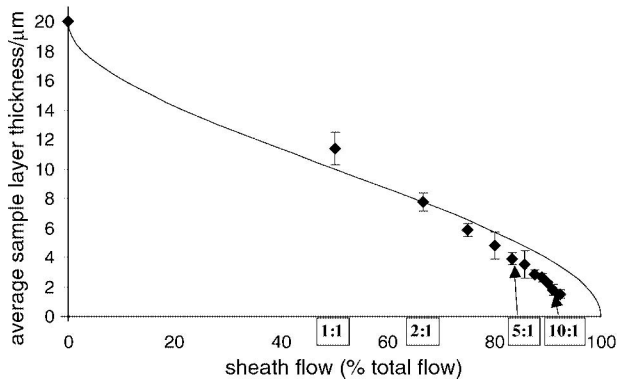

Fig. 8 Average sample layer thickness as a function of sheath flow determined from fluorescence intensities. For a sample flow of 6 μL min^{-1}. Sheath flow is plotted as percentage of total flow (sample + sheath flow). For selected data points the corresponding ratios of sheath to sample flow are also indicated. Measurement values based on three experiments performed on different days with same 3D-microchip. Standard deviations < 1.1 μm. The solid line represents eqn. (3).

Interestingly, the results indicate that the average sample layer thickness depends approximately linearly on the sheath flow rate over the whole measurement range. Considering that pressure driven flow is used, resulting in a parabolic flow profile, this relationship should be non-linear. At a given volume flow rate, a flow confined to the vicinity of a surface forms relatively thicker layers to compensate for the lower velocity. The parabolic velocity profile in a planar flow cell of height H is

$$v(z) = \frac{4v_0 z}{H^2}(H - z) \quad (1)$$

with v_0 the maximum velocity.The volume flow rate per unit width of a flow layer between $z = 0$ and $z = d$ is

$$Q(d) = \int_0^d v(z)\mathrm{d}z \quad (2)$$

from which the sample flow divided by the total flow becomes

$$q(d) = \frac{Q(d)}{Q(H)} = 3\frac{d^2}{H^2} - 2\frac{d^3}{H^3} \quad (3)$$

The corresponding sheath flow divided by the total flow [1 − $q(d)$] is plotted in Fig. 8. The discrepancy may be related to the non-uniform lateral distribution of the sample flow in the sensor cell.

Summary and conclusion

A novel modular microfabrication approach based on PDMS building blocks was tested by applying it to a 3D-microchip for sheath flow applications. Molding of the individual building blocks was performed in a special molding dish which allowed for alignment and joining of up to three masters. The building block quality was found to be satisfactory with proper microstructuring and planar surfaces on up to three sides. An assembled 3D-microchip with plasma-bonded bottom layer proved highly durable over the course of one year. Flow rates of 120 μL min^{-1} (1 cm s^{-1}) were routinely applied without sealing problems. For 3D sheath flow experiments 100 μM fluorescein at 6 μL min^{-1} was used as sample flow and water at increasing flow rates as sheath flow. The resulting sample layer thickness was determined with a simple procedure based on volume detection on an epi-fluorescence microscope and image analysis. With ratios of sheath to sample flow up to 20 : 1 sample layers down to 1 μm thickness could be generated. The results indicate that the average sample layer thickness varies approximately linearly with the sheath flow rate over the whole measurement range. Day-to-day reproducibility was found to be good with standard deviations for sampler layer thickness below ±1 μm for higher sheath flows. The 3D-microchip with its sheath flow channel system can be applied to optical biosensors to enhance mass transport.[32] The main practical advantage is the simple adhesion-based interfacing which allows for cleaning, reuse and transfer of the 3D-microchip. But the modular construction approach could also be applied to the fabrication of laminar micromixers, microchannel separation systems with high sensitivity absorbance detection (with vertical channel extension), or even complete μTAS devices.

Acknowledgement

The authors thank Dr Giles Sanders (Imperial College) for useful discussions.

References

1 S. C. Terry, J. H. Jerman and J. B. Angell, *IEEE Trans. Electron Devices*, 1979, **26**, 1880.
2 S. Shoji, M. Esashi and T. Matsuo, *Sens. Actuators*, 1988, **14**, 101.
3 A. Manz, D. J. Harrison, E. Verpoorte and H. M. Widmer, in *Advances in Chromatography*, ed. P. R. Brown and E. Grushka, Marcel Dekker, New York, 1993, vol. 33, p. 1.
4 D. J. Harrison, K. Fluri, K. Seiler, Z. H. Fan, C. S. Effenhauser and A. Manz, *Science*, 1993, **261**, 895.
5 A. A. Woolley and R. A. Mathies, *Anal. Chem.*, 1995, **67**, 3676.
6 G. T. A. Kovacs, *Micromachined Transducers Sourcebook*, WCB/McGraw-Hill, Boston, 1998.
7 *Micro Total Analysis Systems*, ed. A. van den Berg and P. Bergveld, Kluwer Academic, Dordrecht, 1995.
8 *Microsystem Technology in Chemistry and Life Science*, ed. H. Becker and A. Manz, Springer-Verlag, Heidelberg, 1998.
9 E. M. J. Verpoorte, B. H. Vanderschoot, S. Jeanneret, A. Manz, H. M. Widmer and N. F. deRooij, *J. Micromech. Microeng.*, 1994, **4**, 246.★ *Describes a stacking concept based on photolithographically fabricated silicon discs with channel structuring and through-holes. Several 3D microflow systems are proposed for μTAS applications.*
10 C. Gonzales, S. D. Collins and R. L. Smith, *Sens. Actuators, B*, 1998, **49**, 40.
11 A. Bertsch, H. Lorenz and P. Renaud, *Sens. Actuators, A*, 1999, **73**, 14.
12 B. H. Cumpston, S. P. Ananthavel, S. Barlow, D. L. Dyer, J. E. Ehrlich, L. L. Erskine, A. A. Heikal, S. M. Kuebler, I. Y. S. Lee, D. McCord-Maughon, J. Q. Qin, H. Rockel, M. Rumi, X. L. Wu, S. R. Marder and J. W. Perry, *Nature*, 1999, **398**, 51.
13 J. C. McDonald, D. C. Duffy, J. R. Anderson, D. T. Chiu, H. K. Wu, O. J. A. Schueller and G. M. Whitesides, *Electrophoresis*, 2000, **21**, 27.
14 C. S. Effenhauser, G. J. M. Bruin, A. Paulus and M. Ehrat, *Anal. Chem.*, 1997, **69**, 3451.
15 H. P. Chou, C. Spence, A. Scherer and S. Quake, *Proc. Natl. Acad. Sci. U. S. A.*, 1999, **96**, 11.
16 G. Ocvirk, M. Munroe, T. Tang, R. Oleschuk, K. Westra and D. J. Harrison, *Electrophoresis*, 2000, **21**, 107.
17 Y. Xia, E. Kim, X. M. Zhao, J. A. Rogers, M. Prentiss and G. M. Whitesides, *Science*, 1996, **273**, 347.
18 E. Delamarche, A. Bernard, H. Schmid, B. Michel and H. Biebuyck, *Science*, 1997, **276**, 779.
19 D. C. Duffy, J. C. McDonald, O. J. A. Schueller and G. M. Whitesides, *Anal. Chem.*, 1998, **70**, 4974.★ *Introduces a rapid prototyping procedure for PDMS molding. Master fabrication is based on exposure of a photoresist through a printed transparency with the channel layout. Plasma treatment of PDMS surfaces is employed to temporarily increase the hydrophilicity, and for permanent bonding between PDMS layers.*
20 E. D. L. Eteshola, *Sens. Actuators, B*, 2001, **72**, 129.
21 E. Kim, Y. Xia and G. M. Whitesides, *Nature*, 1995, **376**, 581.
22 R. J. Jackman, D. C. Duffy, E. Ostuni, N. D. Willmore and G. M. Whitesides, *Anal. Chem.*, 1998, **70**, 2280.
23 W. Budach, A. P. Abel, A. E. Bruno and D. Neuschafer, *Anal. Chem.*, 1999, **71**, 3347.
24 E. Delamarche, A. Bernard, H. Schmid, A. Bietsch, B. Michel and H. Biebuyck, *J. Am. Chem. Soc.*, 1998, **9**, 500.
25 B.-H. Jo and D. J. Beebe, *SPIE*, 1999, **3877**, 222.★★ *3D-PDMS approach based on compression molding of thin layers between a SU-8 master and a transparency film. Assembly is facilitated by self alignment between layers via surface tension effects.*
26 B. H. Jo, L. M. Van Lerberghe, K. M. Motsegood and D. J. Beebe, *J. Microelectromech. Syst.*, 2000, **9**, 76.
27 J. R. Anderson, D. T. Chiu, R. J. Jackman, O. Cherniavskaya, J. C. McDonald, H. K. Wu, S. H. Whitesides and G. M. Whitesides, *Anal. Chem.*, 2000, **72**, 3158.★ *3D-PDMS approach based on compression molding between SU-8 and PDMS masters. Yields thin layers with microstructuring on two sides and through-holes. Complex microstructures are realised by sandwiching one or more such layers between thicker support slabs.*
28 D. T. Chiu, N. L. Jeon, S. Huang, R. S. Kane, C. J. Wargo, I. S. Choi, D. E. Ingber and G. M. Whitesides, *Proc. Natl. Acad. Sci. U. S. A.*, 2000, **97**, 2408.
29 F. Zarrin and N. J. Dovichi, *Anal. Chem.*, 1985, **57**, 2690.★ *Early work on employing sheath flow for adjusting detection volumes in a flow cuvette. By introducing a sample flow into the centre of a sheath flow thin sample streams are generated. Theory describing the sample stream radius as a function of sheath and sample flow rates is presented.*
30 D. Sobek, A. M. Young, M. L. Gray and S. D. Senturia, *Proceedings of the 6th IEEE workshop on Micro Electro Mechanical Systems (MEMS '93), Fort Lauderdale, February 7–10*, 1993, pp. 219–224.
31 K. Tashiro, T. Sekiguchi, S. Shoji, T. Funatsu, W. Masumoto and H. Sato, in *Micro Total Analysis Systems 2000*, ed. A. Vandenberg and P. Bergveld, Kluwer Academic, Dordrecht, 2000.
32 O. Hofmann, G. Voirin, P. Niedermann and A. Manz, in *Micro Total Analysis Systems 2001*, ed. J. M. Ramsey and A. Vandenberg, Kluwer Academic, Dordrecht, 2001, pp. 133–134.
33 O. Hofmann, G. Voirin, P. Niedermann and A. Manz, 2001, in preparation.
34 G. L. Duveneck, E. Verpoorte, P. Oroszlan, M. Pawlak, C. Erbacher, A. Spielmann, D. Neuschaefer and M. Ehrat, *Analytical Methods & Instrumentation; Special Issue μTAS '96*, 1996, 158.
35 F. G. Bessoth, A. J. deMello and A. Manz, *Anal. Commun.*, 1999, **36**, 213.
36 J. S. Ploem and H. J. Tanke, *Introduction to fluorescence microscopy (Microscopy handbooks 10)*, Oxford University Press, Oxford, 1987.
37 J. James, *Light microscopic techniques in biology and medicine*, M. Nijhoff, Medical Division, The Hague, 1976.